GeoAmericas2020
4th PAN AMERICAN CONFERENCE ON GEOSYNTHETICS
26-29 APRIL 2020 • RIO DE JANEIRO • BRAZIL

Full-scale testing of geogrid-stabilised aggregate working platforms under controlled loading conditions

Marcotte, B[1], Soliman, H[1], Hammerlindl, A[1], Fox, B[1], Andree, M[1], Howse, K[1], Leik, A[1], Lees, A[2], Wayne, M[2], Kawalec, J[2], Fleming, I.[1]

[1] University of Saskatchewan, Saskatoon, Canada

[2] Tensar International (Various locations)

ABSTRACT

Stabilisation of aggregate layers over weak subgrade soils is frequently accomplished using geogrid for unpaved roads, working platforms, or foundations. The performance of various stabilised aggregate layers over a soft silty clay subgrade soil was evaluated at full scale under highly controlled loading conditions. In order to provide the required reaction load, a moveable loading platform was constructed onto which 4 loaded gravel trucks could be driven. The overall system consisted of a moveable steel load platform that was placed over a trench within which multiple test pads were constructed with different combinations of gravel, thickness and geogrid layers.

Load was applied to a 1m^2 plate area by a hydraulic piston capable of reaching well over 1000 kN, thus representing loading fully at field scale. All tests were taken past ultimate bearing capacity failure to a maximum stroke of 250 mm. A photogrammetric procedure was developed to define in 3 dimensions the deformed surfaces of the gravel surface and the interface with the soft clay subgrade below. The photogrammetry procedure yields digital elevation models, which clearly illustrate the nature of the displacement of the ground surface, the geogrid reinforcement, and the aggregate – subgrade interface. The variations in the precise pattern of deformation serve to highlight aspects of the aggregate – geogrid interaction and serve to highlight the specific soil-geogrid interaction behaviour. Combined with future numerical modelling back-analyses, the data from these full-scale tests will contribute to an improved understanding of the interactions between the clayey subgrade, the stabilising geogrid and the aggregate.

1. INTRODUCTION

Geogrids can be used to increase the bearing capacity of aggregate working platforms or access roads over weak soils. The geogrid can increase the load that can be supported by a given thickness of aggregate base material, or reduce the amount of base material required for a given load. The use of geogrids can prolong the lifespan of roads, reduce the required maintenance, or prevent costly bearing capacity failures when supporting heavy equipment.

The geogrid can perform its support function as either a tensioned membrane (Giroud et al. 1985), or, as has been increasingly demonstrated, by stabilising the aggregate layer (Byun et al. 2019; Dobie et al. 2019). The principles underlying the tension membrane mechanism differ from those for stabilisation in that large strains (significant rutting) are required to develop strength. The stabilisation mechanism is based on the geogrid interlocking with particles to constrain particle movement or rotation with resultant increase of both stiffness and shear strength of the aggregate in the vicinity of the geogrid (Tutumluer et al. 2012; Lees & Clausen 2019). The efficiency of the geogrid to effect stabilisation depends on geogrid properties such as aperture, small strain tensile modulus, and the ability to interlock with the aggregate material. The geogrid stabilisation effect has been successfully numerically modeled by altering the soil material parameters (c' method) around the location of the geogrid to account for the stabilisation effect (Lees, 2017b; Lees & Clausen 2019) rather than as a membrane or bar element. Better agreement between physical and numerical models using the c' method have contributed into further understanding of the mechanism of geogrid stabilisation.

Through stabilisation, the granular layer tends to resist punching shear failure. The transfer of load from the base to the subgrade is distributed wider, reducing the pressure on the soil below (Dobie et al. 2018). This mechanism in turn forces any bearing capacity failure deeper into the subgrade soil, effectively increasing the bearing capacity of the multi-layered system (Laman et al. 2012).

Numerous studies have evaluated increased strength and stiffness from geogrids in a laboratory setting (Mekkawy et al. 2011; Byun et al. 2019; Abu-Farsakh et al. 2016; Qian et al. 2013). Geogrid apertures typically range from 30

mm to 50 mm, which make it difficult to conduct full-scale laboratory testing without significant boundary effects due to limitations on load plate sizes. A large scale field test (0.64m^2) conducted by Laman et al. (2012) provided data on load displacement, however, the load was not controlled and surface displacements were not measured.

This study presents the findings from a large, 1m^2, plate load test on geogrid stabilised aggregate over a soft clayey subgrade. In each test, the gravel or geogrid stabilised gravel was taken past bearing capacity failure. Comparison of the deformed surfaces of the aggregate and clay surfaces are performed to demonstrate the load-transfer mechanism of the geogrid to effectively increasing the punching shear failure.

2. CONSTRUCTION OF LARGE LOADING DEVICE

The objectives of the study were to evaluate and compare geogrid stabilised to non-stabilised aggregate during controlled loading. To accomplish multiple large-scale tests, a relatively uniform subgrade soil was found and charecterised in Saskatchewan, Canada. Multiple Shelby tube samples, dual cone penetrometer, and cone penetration tests (CPT) were conducted as shown in the diagram in Figure 1. Currently, shear vane testing and additional CPT tests are underway. The undrained shear strength of the soil was relatively constant and it is estimated that it varied from 50 kPa to 30 kPa from one side of the test pad to the other.

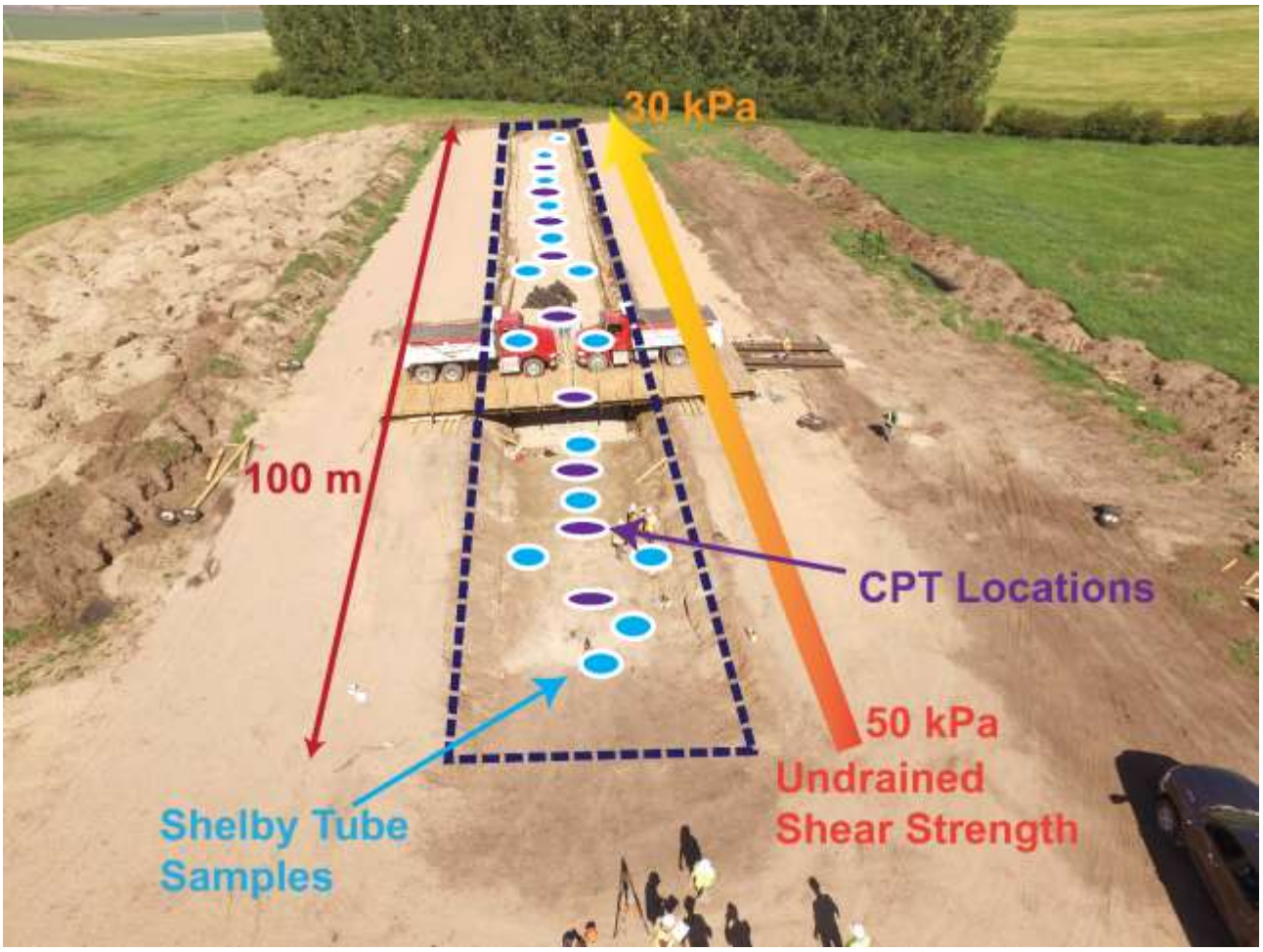

Figure 1: Diagram of test program and location of samples

Due to the weak surrounding soil, limit equilibrium modelling of the test set-up demonstrated that the sides of the test pad trench required reinforcement to support the load of the reaction frame. The reinforced sidewalls consisted of two layers of geogrid with a nonwoven geotextile wrapped face with gravel backfill as shown in Figure 2 (left) and in Figure 3. Once the reinforced sidewalls were constructed, an excavator dug the trench from the reinforced sidewalls so as to avoid trafficking on the uniform soft clayey soil to be tested. Gravel and geogrid were then placed using low ground pressure equipment. A total of 18 test pads were constructed.

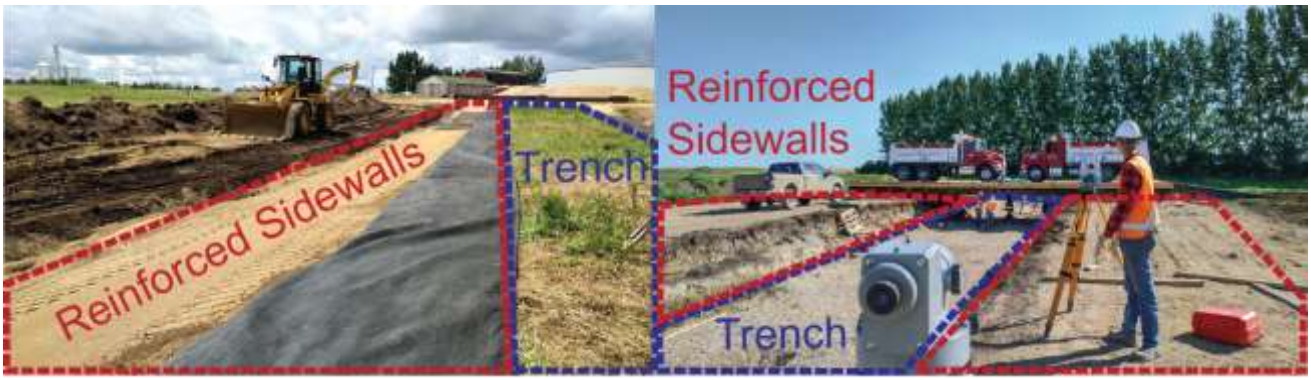

Figure 2: Construction of test pad trench and reinforced walls

The reaction load frame had to be heavy enough to push up to 50 cm of gravel and geogrid above the soft clay soil below into bearing capacity failure. On the other hand, it had to be mobile to move along the trench to different test configurations. A large load frame was constructed at the University of Saskatchewan as shown in Figure 3. A hydraulic cylinder mounted to the underside of the reaction frame provided the load to the reinforced 1m^2 plate – which could be controlled on the basis of either displacement rate or measured load.

Figure 3: Constructed steel load platform with loaded gravel trucks above

Heavy timber decking was placed over the steel frame to support the loaded gravel trucks. Movable steel ramps provided access for up to four loaded gravel rock trucks to drive onto the load frame. The load frame was dragged between successive test locations on wooded skids using heavy equipment. The weight of the load frame provided 166 kN of reaction force. With the loaded gravel trucks above the reaction force was over 1150 kN.

To ensure no eccentric forces were transferred to the load cell, a rather elaborate loading attachment was constructed as shown in Figure 4.

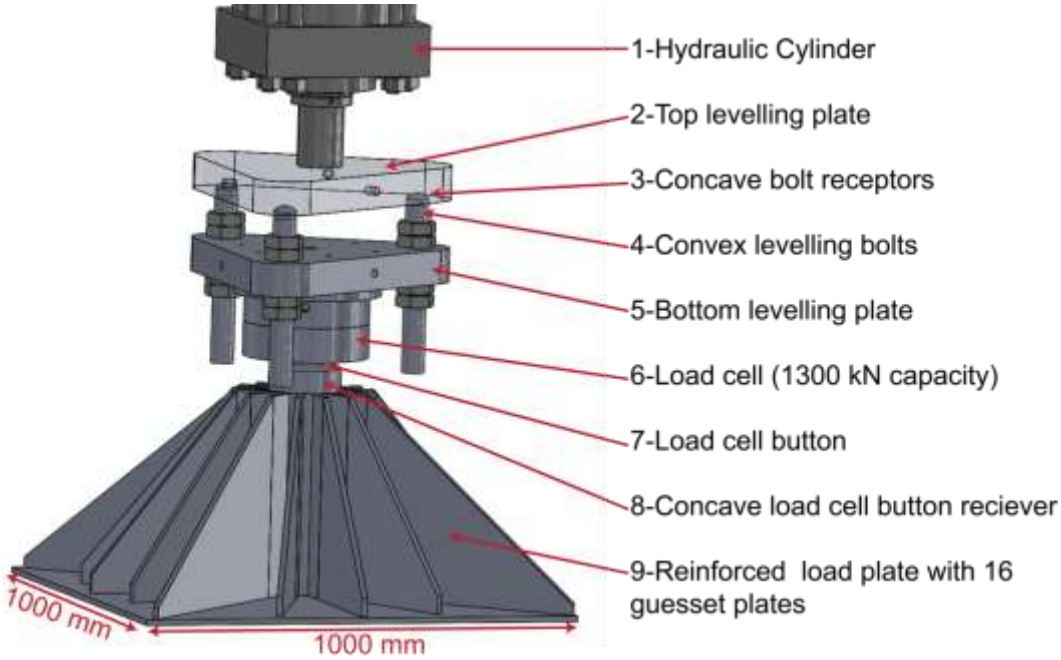

Figure 4: Loading plate assembly and levelling system

The piston from the pneumatic cylinder (1) threaded into a large, custom built thick steel triangular plate (2). On the underside of the plate, concave grooves (3) were machined to match the large bolts (4). A second triangular plate was machined to fit the three bolts while also attaching the load cell below (5). This custom "tri-brach" assembly allowed for precise adjustments and levelling of the load cell assembly (6) to ensure force was directed vertically through the load cell to the load plate without inducing plate rotation. The mounting surface of the load plate (8) was machined concave to ensure good mating with the convex load button (7). The load plate (9) was constructed of thick steel and reinforced with 16 gusset plates to eliminate any bending. This system worked well during all tests as minimal rotation of the plate occurred prior to yielding. The largest post yield rotation that was observed was approximately 6°, most of which occurred after bearing capacity failure. Minimal pre-yield rotation of the plate occurred during testing.

3. PHOTOGRAMMETRY

Photogrammetry is the science of taking measurements from photographs (Mikhail et al. 2001). The pixel data captured by the camera sensor can be triangulated if multiple overlapping images capture similar features or objects. With increases in computing power and camera technology, it is becoming a cost-effective alternative to light detection and ranging (LIDAR) with the added benefit of matching colors with high accuracy.

Photogrammetry was used to measure surface displacements around the plate. The procedure was performed both prior to loading and after loading had commenced but prior to the removal of any load. The photogrammetric process relies on random patterns and pixels to facilitate the matching algorithms. Before the test began, the surface was spray painted in a random fashion as shown in **Error! Reference source not found.**, similar to the laboratory methods developed by Marcotte and Fleming (2019). The grid pattern was not necessary for the photogrammetry, but rather assisted the photographer by providing reference points to ensure good overlap was achieved when capturing images. The achieved overlapping images is shown in Figure 5 (right).

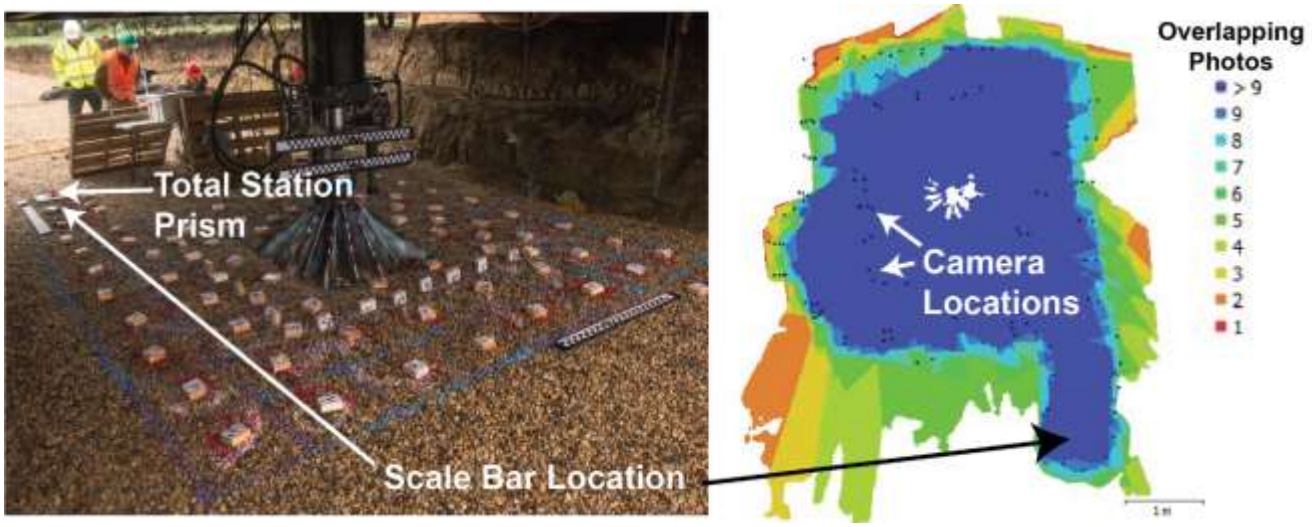

Figure 5: Spray painted surface prior to beginning of test (left); overlap of photographs taken (right)

About 120-140 high resolution RAW images were taken using a fixed focal length single lens reflex digital camera for each model. A custom scale bar was placed within the area being photographed to relate relative distances to real world distance. The scale bar had to be placed approximately 4 metres away from the centre of the load plate to ensure it was not displaced during loading as to provide a fixed location. To confirm that no movement occurred, a total station prism was placed on the scale bar and was checked before and after loading, and no movement occurred during any tests using this procedure.

The photographs were converted to TIFF files and processed using Agisoft's Metashape software (Agisoft 2019). A powerful desktop computer (64 GB ram, 12 virtual cores) processed each set of photographs into a point cloud and mesh in approximately 5 hours on high settings. A point cloud density of 2.5 points/mm^2 was estimated by dividing the surface area of the mesh by the number of points.

The mesh was then reduced to a 1 cm point cloud using a poison-disk sampling technique (Corsini et al. 2012; Cignoni et al., 2008) and then further interpolated and reduced into a 5cm regular grid using a program written in Python. By performing before and after photogrammetry on the gravel surface, the difference could be determined and serves as an estimate of the relative surface displacements. A K-D tree scheme (Murphy and Selkow 1986) was implemented to find the nearest elevation (z) corresponding to a given coordinate (x,y) in the before and after surfaces. A 5 cm spacing was selected as a balance of resolution and processing time – increasing the frequency of points from 5 cm to 3 cm spacing increased the processing time from 2 min to 20 min. The general workflow is shown in Figure 6.

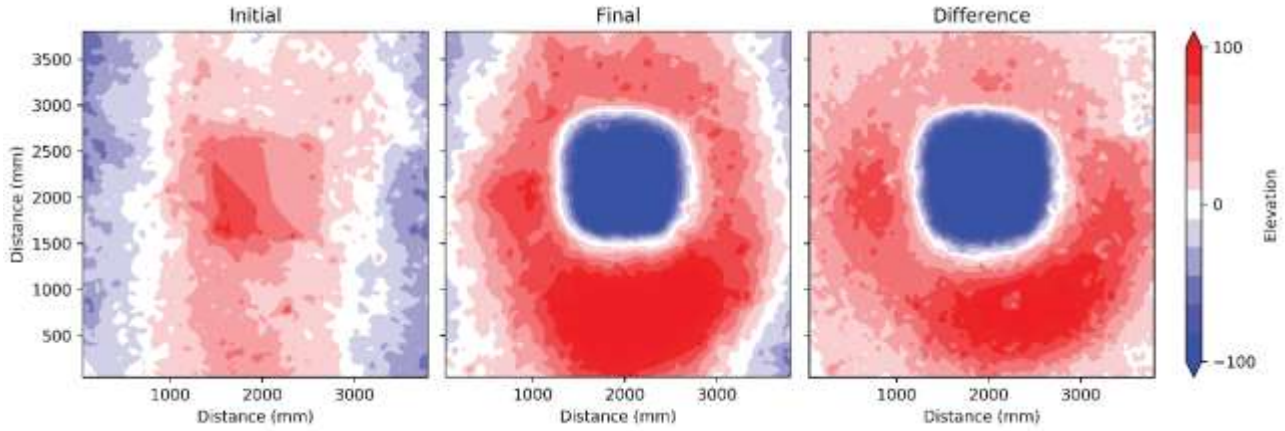

Figure 6: Workflow to determine changes in ground surface elevation during plate load testing

The initial surface and final surfaces appear slightly tapered to the sides indicating that the gravel was not completely level across the width of the trench for this test shown. The zero plane is an arbitrary elevation for the initial and final plots based on the scale bar elevation as shown in Figure 5, and differences in elevation simply reflect that the gravel was higher or lower than the scale bar initially. Heave can clearly be seen while looking at the difference between the initial and final. For the plot labelled "Difference", the zero contours represent areas that no heave occurred. The non-symmetrical pattern of heave in Figure 6 reflects the fact that the geogrid ruptured on one side only, causing the plate to rotate and produce a pronounced heave.

The main purpose of the photogrammetry at the surface was to evaluate the pattern and magnitude of displacement when comparing tests with grid to tests without geogrid (all else being equal). More heave appeared to have occurred in tests with geogrid present, as shown in Figure 7. Displacements were observed at over 2B away from the plate.

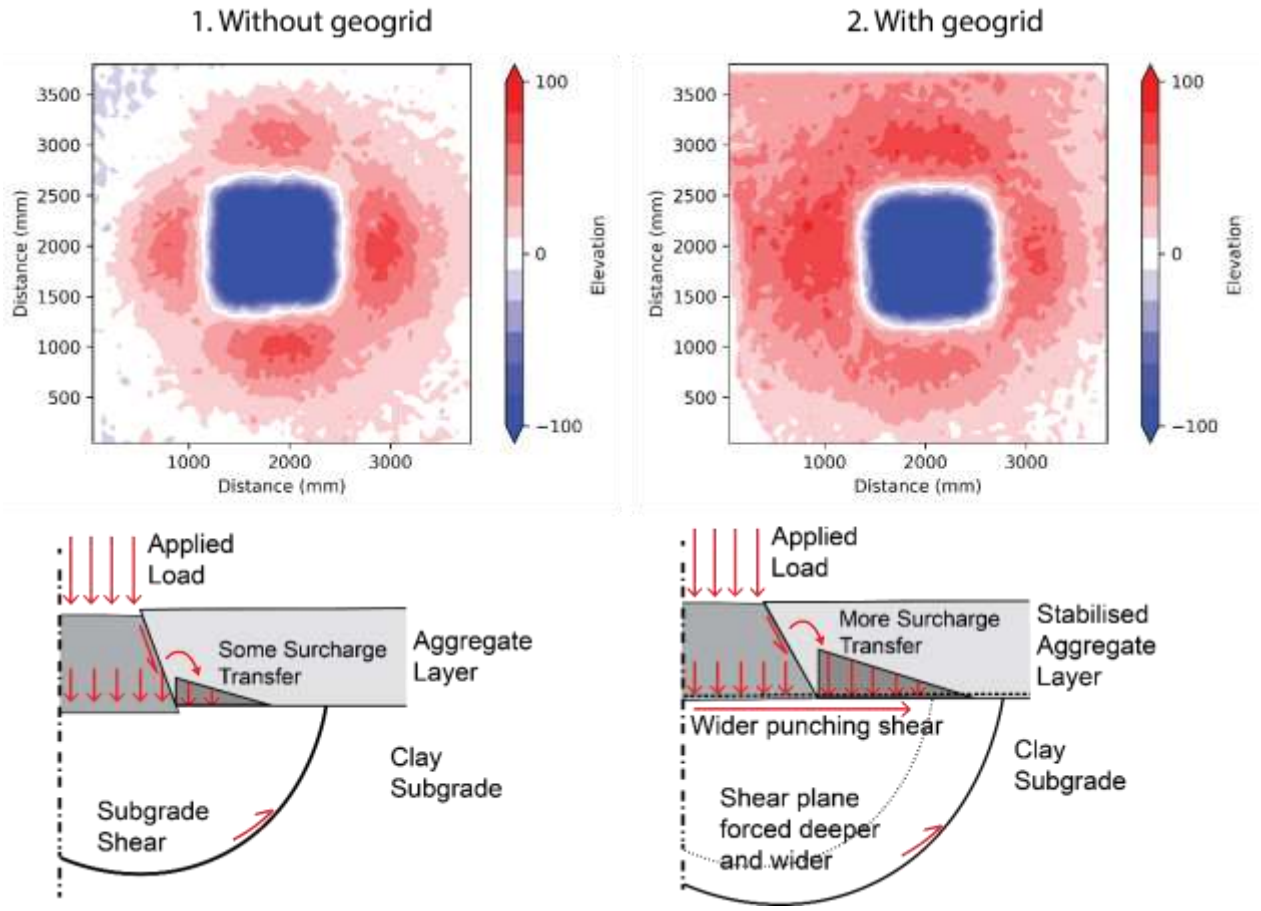

Figure 7: Comparison of gravel surface displacements for tests with and without geogrid and surcharge transfer concept and wider punching shear failure with geogrid (adapted from Lees 2017a,b)

The difference in heave can be explained by the proposed surcharge transfer concept (Lees 2017a). With an increase in surcharge transfer, the shear plane is pushed deeper and wider into the weak clay below. This in turn forces the failure surface wider and the heave at the surface occurs farther from the edge of the plate. Once geogrid rupture occurs, as can be seen on video recordings of the test, the subgrade shear plane reduces and significant heave occurs near the vicinity of the plate post yield as well.

The geogrid was known to have ruptured as a forensic investigation is currently being undertaken by carefully and manually, shoveling out the overlying gravel for each test as shown in Figure 8. Geogrid rupture locations are photographed and mapped.

Figure 8: Forensic investigation uncovering underlying clay surface and geogrid

A photogrammetric procedure was also used to evaluate the shape of the underlying clay surface and geogrid. The photogrammetry procedure was accurate enough to capture details on the geogrid location, aperture size, and rib direction, which will be valuable in future analysis and modelling of the test results. An example of a cross section of the exposed geogrid surface is shown in Figure 9.

Figure 9: Cross section of photogrammetry reproduced geogrid surface and rupture location

The clay surfaces are currently being related to true displacement, similar to the results shown in Figure 6 and Figure 7. Once the displacements are determined, they will then be compared to the surface heave observed in the gravel. The photogrammetric procedure has provided a valuable tool in preserving results which also contains details such as color as to differentiate the geogrid from the gravel.

4. CONCLUSIONS

A large loading device was constructed above a trench cut in soft soil to evaluate multilayered bearing capacity of aggregate with and without geogrid. The project involved numerous unique design challenges such as the portability of the loading device, reinforcement of the trench sidewalls, and distributing the load to the load plate, allowing for measurement by a high-capacity load cell, while avoiding either plate rotation or binding of moving parts. During all tests, the granular layer (stabilised or not) was taken well past yield. Photogrammetry was used during testing and during the forensic analysis as a means to evaluate displacement as well as preserving test details.

Although the results are preliminary, wider surface displacements were observed in the geogrid-stabilised test, which may be indicative that the failure plane was pushed deeper and wider into the weak soil below as expected (Lees 2017a, 2019) The mechanism for the distribution of load is related to the ability of the geogrid to prevent particle rotation or reorientation, thus creating a layer of stiffer composite material in proximity to the geogrid. This in turn increases the bearing capacity by transferring load laterally and forcing the failure surface deeper. Without context, the greater surface displacement may appear unfavourable, but it is in fact the opposite, as the larger displacements appear to confirm the surcharge transfer concept.

Photogrammetry was a useful tool in measuring and evaluating the response of the ground. Before and after photogrammetry can be used to measure differences in elevation with high accuracy. The advantages of photogrammetry over LIDAR is the ability to capture color for each identified point within the point cloud, preserving small details such as the geogrid for further analysis. Work is currently underway to process the force displacement data as well as numerical modelling of the results.

5. AKNOWLEDGMENTS

The authors would like to acknowledge the support of Tensar International Corporation, the University of Saskatchewan's College of Engineering, and the Livestock & Forage Centre of Excellence. The authors would also like to thank all the people that lent a hand outside of their own research projects to help make this project a success.

6. REFERENCES

Agisoft, L. L. C. (2019). Agisoft Metashape User Manual, Professional edition, version 1.5. 2019.

Abu-Farsakh, M. Y., Akond, I., & Chen, Q. (2016). Evaluating the performance of geosynthetic-reinforced unpaved roads using plate load tests. International Journal of Pavement Engineering, 17(10), 901-912.

Byun, Y. H., Tutumluer, E., Feng, B., Kim, J. H., & Wayne, M. H. (2019). Horizontal stiffness evaluation of geogrid-stabilized aggregate using shear wave transducers. Geotextiles and Geomembranes, 47(2), 177-186.

Cignoni, P., Callieri, M., Corsini, M., Dellepiane, M., Ganovelli, F., & Ranzuglia, G. (2008, July). Meshlab: an open-source mesh processing tool. In Eurographics Italian chapter conference (Vol. 2008, pp. 129-136).

Dobie, M., Lees, A., & Khanardnid, J. (2018). Case study: performance of a geogrid stabilised working platform constructed over extremely soft dredged silt. In Proceedings of the 11th International Conference on Geosynthetics, Korea.

Giroud, J. P., Ah-Line, C., & Bonaparte, R. (1985). Design of unpaved roads and trafficked areas with geogrids. Polymer grid reinforcement: proceedings of a conference sponsored by the science and engineering research council and netlon ltd and held in london 22-23 march 1984. Publication of: Telford (Thomas) Limited.

Laman, M., Yildiz, A., Ornek, M., & Demir, A. (2012). Field test of circular footings on reinforced granular fill layer overlying a clay bed. Geotechnical Testing Journal, 35(4), 575-585.

Lees, A. (2017a). Simulation of geogrid stabilization by finite element analysis. In Proceedings of the International Conference on Soil Mechanics and Geotechnical Engineering, Seoul (pp. 1377-1380).

Lees, A. (2017b). Bearing capacity of a stabilised granular layer on clay subgrade. In Proceedings of the 10th International Conference on the Bearing Capacity of Roads, Railways and Airfields (eds. Loizos et al) (pp. 1135-1142).

Marcotte, B. A., & Fleming, I. R. (2019). The role of undrained clay soil subgrade properties in controlling deformations in geomembranes. Geotextiles and Geomembranes, 47(3), 327-335.

Mikhail, E. M., Bethel, J. S., & McGlone, J. C. (2001). Introduction to modern photogrammetry. New York.

Mekkawy, M. M., White, D. J., Suleiman, M. T., & Jahren, C. T. (2011). Mechanically reinforced granular shoulders on soft subgrade: Laboratory and full scale studies. Geotextiles and Geomembranes, 29(2), 149-160.

Murphy, O. J., & Selkow, S. M. (1986). The efficiency of using kd trees for finding nearest neighbors in discrete space. Information Processing Letters, 23(4), 215-218.

Tutumluer, E., Huang, H., & Bian, X. (2010). Geogrid-aggregate interlock mechanism investigated through aggregate imaging-based discrete element modelling approach. International Journal of Geomechanics, 12(4), 391-398.

Qian, Y., Han, J., Pokharel, S. K., & Parsons, R. L. (2012). Performance of triangular aperture geogrid-reinforced base courses over weak subgrade under cyclic loading. Journal of Materials in Civil Engineering, 25(8), 1013-1021.